



Published in final edited form as:

*Langmuir*. 2008 October 7; 24(19): 11293–11299. doi:10.1021/la8017634.

## Parallel Arrays of Geometric Nanowells for Assembling Curtains of DNA with Controlled Lateral Dispersion

Mari-Liis Visnapuu<sup>‡,§</sup>, Teresa Fazio<sup>†,§</sup>, Shalom Wind<sup>†</sup>, and Eric C. Greene<sup>\*,‡</sup>

<sup>†</sup>Department of Applied Physics and Applied Mathematics, Center for Electron Transport in Molecular Nanostructures, NanoMedicine Center for Mechanical Biology, Columbia University 1020 Schapiro CEPSR, 530 West 120th Street, New York, New York 10027

<sup>‡</sup>Department of Biochemistry and Molecular Biophysics, Columbia University, 650 West 168th Street, Black Building Room 536, New York, New York 10032

### Abstract

The analysis of individual molecules is evolving into an important tool for biological research, and presents conceptually new ways of approaching experimental design strategies. However, more robust methods are required if these technologies are to be made broadly available to the biological research community. To help achieve this goal we have combined nanofabrication techniques with single-molecule optical microscopy for assembling and visualizing curtains comprised of thousands of individual DNA molecules organized at engineered diffusion barriers on a lipid bilayer-coated surface. Here we present an important extension of this technology that implements geometric barrier patterns comprised of thousands of nanoscale wells that can be loaded with single molecules of DNA. We show that these geometric nanowells can be used to precisely control the lateral distribution of the individual DNA molecules within curtains assembled along the edges of the engineered barrier patterns. The individual molecules making up the DNA curtain can be separated from one another by a user-defined distance dictated by the dimensions of the nanowells. We demonstrate the broader utility of these patterned DNA curtains in a novel, real time restriction assay that we refer to as dynamic optical restriction mapping, which can be used to rapidly identify entire sets of cleavage sites within a large DNA molecule.

### Introduction

Advances in biology are often made possible only through the concurrent establishment of new technologies that bring together different scientific disciplines to achieve a common goal. This maxim has proven especially true for single-molecule research, where aspects of physics, chemistry, and biology have all provided invaluable contributions, which have led to the development of highly sensitive detection optics, robust fluorescent tags, and novel chemistries for anchoring individual molecules to surfaces. Taken together, these technological achievements have enabled new approaches for isolating, viewing and manipulating individual macromolecules while at the same time addressing important biological questions. Nowhere is this trend more evident than in the study of nucleic acids and protein—nucleic acid interactions.<sup>1-5</sup> Yet even as these approaches continue to illuminate specific reaction mechanisms, broader implementation of the techniques remains hindered by low throughput

capacity and challenging technical nature; as a consequence most studies have been restricted to relatively simple model systems implemented by a handful of specialized laboratories.

In an effort to help make these techniques more accessible we have integrated nanoscale engineering, microfluidics, and inert lipid bilayer-coated surfaces with optical microscopy to develop novel high-throughput methods for making curtains of DNA molecules that can be used for massively parallel data acquisition from thousands of individual protein—DNA complexes in real time using a robust experimental platform that is amenable to a wide variety of biological applications.<sup>6,7</sup> Our initial studies utilized manual etching to make microscale barriers to lipid diffusion, which in turn could be used to align hundreds of lipid-tethered DNA molecules.<sup>7</sup> More recently we have established methods for nanofabricating chromium (Cr) barriers that allow for much more precise control over the location of the DNA.<sup>6</sup> These DNA curtains permit simultaneous visualization of thousands of individual DNA molecules that are perfectly aligned with respect to one another. This setup is especially applicable to the real time detection of fluorescent proteins bound to the DNA.<sup>8-11</sup> However, a remaining limitation of this approach is the lack of control over the lateral separation between each of the molecules making up the DNA curtains. This can potentially present a problem, especially in instances where either implementation of the desired experiments or the subsequent data analysis is confounded by the presence of overlapping molecules within the curtain. In addition, the DNA molecules tend to slip laterally along the chromium barrier edges, an effect that is most obvious with lower DNA densities and/or shorter molecules of DNA. The lipid bilayers remain fluid at the edges of the chromium barriers,<sup>12</sup> and the observed mobility of the DNA arises from slippage of the lipid anchors along the smooth barrier edges. This can be problematic for single molecule data analysis because molecules targeted for investigation will inevitably slip along the barrier edge and collide with and/or bypass one another, making it extremely difficult to distinguish similar looking molecules from one another over periods longer than just a few seconds. Taken together, these complications can place significant design constraints on the experiments that can be conducted with DNA curtains, especially when using DNA substrates shorter in length than the phage  $\lambda$  genome.

Here we sought to develop new barrier designs that could control the positions of the molecules within the DNA curtain. We take advantage of the fact that lipid-tethered DNA molecules can slide along the barrier edges by demonstrating that simple geometric barrier patterns made by nanolithography can be used to generate aligned DNA curtains with precisely controlled lateral displacement between the molecules. These barriers consist of a repetitive triangular wave (sawtooth pattern) with nanometerscale features, where the vertex of each adjacent triangle forms a tiny well, which we will refer to as geometric nanowells. We show that single molecules of DNA can be loaded into the nanowells and retained for observation and analysis. The minimal separation distance between each of the DNA molecules within the curtain is defined by the distance between the adjacent nanowells within the geometric barrier pattern, and the total number of DNA molecules within in each well is controlled by the amount of DNA applied to the surface. Although designed explicitly for single-molecule biochemical studies of protein-DNA interactions, DNA curtains made with these geometric barrier patterns have other potential applications. As an example of their broader utility, we use the DNA curtains made with geometric nanowells in a novel dynamic optical restriction mapping assay, which uses real time data collection to identify an entire set of specific cleavage sites within the phage  $\lambda$  genome in a reaction that takes under 2 min.

## Materials and Methods

### Barrier Construction by E-Beam Lithography

Fused silica slides were cleaned in NanoStrip solution (CyanTek Corp, Fremont, CA) for 20 min, then rinsed with acetone and isopropanol and dried with N<sub>2</sub>. The slides were spin-coated

with a bilayer of polymethylmethacrylate (PMMA), molecular weight 25 K, 3% in anisole and 495 K, 1.5% in anisole (MicroChem, Newton, MA), followed by a layer of Aquasave conducting polymer (Mitsubishi Rayon). Each layer was spun at 4000 rpm for 45 s using a ramp rate of 300 rpm/s. Patterns were written by E-beam lithography using an FEI Sirion scanning electron microscope equipped with a pattern generator and lithography control system (J. C. Naby, Inc., Bozeman, MT). After patterning, Aquasave was rinsed off with deionizing water. Resist was developed using a 3:1 solution of isopropanol to methyl isobutyl ketone (MIBK) for 2 min with ultrasonic agitation at 5 °C. The substrate was then rinsed in isopropanol and dried with N<sub>2</sub>. A thin layer of chromium was deposited using a Semicore electron beam evaporator. To effect lift-off, the coated substrate was submerged in a 65 °C acetone bath for 30 min, and then gently sonicated. Following lift-off, samples were rinsed with acetone to remove stray chromium flakes and dried with N<sub>2</sub>. Barriers were imaged using a Hitachi 4700 scanning electron microscope and a PSIA XE-100 Scanning Probe Microscope in noncontact mode. Optical images of the barriers were taken with a Nikon Eclipse ME600 at either 10× or 20× magnification (as indicated).

### Lipid Bilayers and DNA Curtains

The flowcells were assembled from fused silica slides (G. Finkenbeiner, Inc.) with chromium nanoscale diffusion barriers. Inlet and outlet ports were made by boring through the slide with a high-speed precision drill press equipped with a diamond-tipped bit (1.4 mm O.D.; Kassoy). The slides were cleaned by successive immersion in 2% (v/v) Hellmanex, 1 M NaOH, and 100% MeOH. The slides were rinsed with filtered sterile water between each wash and stored in 100% MeOH until use. Prior to assembly, the slides were dried under a stream of nitrogen and baked in a vacuum oven for at least 1 h. A sample chamber was prepared from a borosilicate glass coverslip (Fisher Scientific) and double-sided tape (~25 μm thick, 3M). Inlet and outlet ports (Upchurch Scientific) were attached with hot-melt adhesive (Sure-Bonder glue sticks, FPC Corporation). The total volume of the sample chambers was ~4 μL. A syringe pump (Kd Scientific) and actuated injection valves (Upchurch Scientific) were used to control sample delivery, buffer selection and flow rate. The flowcell and prism were mounted in a custom-built heater with computer-controlled feedback regulation to control the temperature of the sample from between 25-37 °C (±0.1 °C), as necessary.

DNA curtains were constructed as described.<sup>7</sup> All lipids were purchased from Avanti Polar Lipids and liposomes were prepared as previously described. In brief, a mixture of DOPC (1,2-dioleoyl-*sn*-glycero-phosphocholine), 0.5% biotinylated-DPPE (1,2-dipalmitoyl-*sn*-glycero-3-phosphoethanolamine-*N*-(cap biotinyl)), and 8% mPEG 550-DOPE (1,2-dioleoyl-*sn*-glycero-3-phosphoethanolamine-*N*-[methoxy(polyethylene glycol)-550]). The mPEG is does not affect bilayer formation or assembly of the DNA curtains, but rather serves to further passivated the surface against nonspecific adsorption of quantum dots (which we use in our studies of protein-DNA interactions).<sup>8</sup> Liposomes were applied to the sample chamber for 30 min. Excess liposomes were flushed away with buffer containing 10 mM Tris-HCl (pH 7.8) and 100 mM NaCl. The flowcell was then rinsed with buffer A (40 mM Tris-HCl (pH 7.8), 1 mM DTT, 1 mM MgCl<sub>2</sub>, and 0.2 mg/mL BSA) and incubated for 15 min. Neutravidin (660 nM) in buffer A was then injected into the sample chamber and incubated for 10 min. After rinsing thoroughly with additional buffer A, biotinylated (±DNA (10 pM) prestained with 1-2 nM YOYO1 was injected into the sample chamber, incubated for 10 min, and unbound DNA was removed by flushing with buffer at 0.1 mL/min. Application of buffer flow caused the lipid-tethered DNA molecules to align along the leading edges of the diffusion barriers. The flow was stopped for 5 min allowing the DNA to diffuse toward the center of the barriers. The flow was started at 0.1 mL/min for 30 s and the flow on-off cycle was repeated 3-5 times until DNA curtains of even density formed along the diffusion barriers.

## TIRFM Imaging

The basic design of the microscope used in this study has been previously described.<sup>11</sup> In brief, the system is built around a Nikon TE2000U inverted microscope with a custommade illumination system. For this study, a 488 nm, 200 mW diodepumped solid-state laser (Coherent, Sapphire-CDHR) was used as the excitation source. The laser was attenuated as necessary with a neutral density filter and centered over the DNA curtain by means of a remotely operated mirror (New Focus). The beam intensity at the face of the prism was typically ~10-15 mW. Images were detected with a back-illuminated EMCCD detector (Photometrics, Cascade 512B). TIRFM images were collected using a 60× water immersion objective lens (Nikon, 1.2 NA Plan Apo), unless otherwise indicated.

## Results

### Design Strategy

We have shown that mechanical barriers to lipid diffusion can be used to organize DNA molecules into curtains that serve as a unique and effective experimental platform for the study protein-DNA interactions at the single molecule level.<sup>6-11</sup> DNA molecules are first anchored by one end to a supported lipid bilayer coating the surface of the sample chamber and application of hydrodynamic force is used to push the lipidtethered DNA molecules toward the lipid diffusion barriers. Lipids within supported bilayers can not traverse these mechanical barriers.<sup>13-15</sup> As a consequence the barriers also halt the forward movement of the DNA molecules, causing them to accumulate at the barrier edges where they extend into the evanescent field (Figure 1).

DNA molecules can diffuse laterally along the smooth edges of the Cr barriers and the magnitude of this movement can be quite substantial (see below). This is because the lipid bilayers remain fluid even at the barrier edges,<sup>12</sup> and the tension exerted on the DNA molecules by the hydrodynamic force is insufficient to overcome the tendency of the molecules to slide along the barriers. This becomes especially problematic with shorter DNA molecules. In addition, these chromium barriers are oriented perpendicular to the flow force, but if they are misaligned by just a few degrees relative the direction flow, then the DNA molecules slip rapidly along the barrier edges (data not shown). In light of these potential issues, we sought a new barrier design that could eliminate slippage of the molecules along the barrier edges. We reasoned that the locations of the DNA molecules along the barrier edges could be passively controlled by altering the shape of the barriers themselves. For example, because the DNA molecules can move along the smooth barrier edges then, geometric barrier patterns comprised of a simple, repetitive triangular wave would limit the mobility (Figure 1B and C). This is because the hydrodynamic force exerted by the flowing buffer should push the DNA molecules into the vertex of each triangle with sufficient force to overcome any tendency of the molecules to move laterally within the bilayer (Figure 1B and C). We refer to these triangular features as geometric nanowells because the DNA molecules loaded within each well would not be free to move laterally along the barrier, as long as a continuous flow force is maintained. In addition to eliminating lateral slippage, we also expected that the peak-to-peak distance of the adjacent triangles within the patterns would dictate the minimal lateral separation of the DNA molecules that make up the curtain. For example, geometric patterns that repeat at 500 nm intervals should yield DNA molecules separated from one another by 500 nm. The separation will be greater than 500 nm if some of the wells are not occupied, yet even in this case the distances should occur in defined increments divisible by 500 nm (i.e., 500, 1000, 1500, 2000 nm, etc.). If this is true, then these geometric barrier patterns will confer precise control over the positioning of each individual DNA making up the curtain.

Examples of the geometric barrier patterns tested here are shown in Figure 2. We used electron-beam (E-beam) lithography to achieve these desired design features by engineering chromium barriers that were typically 100 nm wide and 20 nm tall arranged in a sawtooth pattern on a fused silica slide. Figure 2A shows an optical image of a pair of barrier sets and once assembled into a flowcell the chromium barriers will be oriented perpendicular to the hydrodynamic force with the apex of each triangle pointing in the same direction that the buffer is flowing (as indicated in Figure 1). Figure 2B shows an AFM image of a geometric barrier pattern with 1  $\mu\text{m}$  peak-to-peak spacing and reveals a height of just 20 nm. Examples of SEM images of geometric barriers with peak-to-peak distances of 1900, 1000, 750, 500, 350, and 200 nm are shown in Figure 2C-H. These images demonstrate that we can use standard lithographic techniques to construct chromium barriers with precise geometric patterns having nanometer scale features of our desired designs.

### DNA Curtains with Defined Lateral Separation between Molecules

Figure 3A-D shows representative examples of YOYO1-stained DNA curtains assembled at a barrier pattern with either 1000 nm spacing (A and B) or 1900 nm spacing (C and D) between the adjacent geometric nanowells. In the presence of buffer flow the DNA molecules are extended along the surface, but when flow is terminated they diffuse out of view, verifying that they are not nonspecifically adsorbed to the bilayer. These images demonstrate that the geometric barrier patterns can be used to prepare DNA curtains, and also shows that the distance between the DNA molecules is influenced by the spacing constraints of the nanowells (compare A and C). If the DNA molecules within the curtains were in fact retained within the geometric nanowells, as we predicted, then the distance between the adjacent vertices of triangles within the pattern design should be reflected in the separation distance between the individual DNA molecules. Figure 3E highlights examples of DNA curtains made with geometric barrier patterns with 1900, 1000, 750, 500, 350, and 200 nm separation between adjacent nanowells. These curtains are comprised of the 23 kb DNA that is fluorescently stained with the intercalating dye YOYO1. To verify that this design pattern yielded DNA molecules with the desired spacing we plotted signal intensity of the stained DNA versus its lateral location along the barrier edge, and these plots confirmed peak-to-peak distances consistent with values expected from designs of the geometric barrier patterns (Figure 3F). As expected, the 1900, 1000, 750, 500, 350, and 200 nm barriers yielded separation distances corresponding to the pattern designs. For the geometric nanowells with 1900, 1000, 750, 500, and 350 nm spacing we could resolve the distances between DNA molecules loaded into adjacent wells. For the 200 nm nanowells spacing it was not possible to resolve DNA molecules loaded into adjacent wells because the closely spaced molecules led to overlapping fluorescence signal. However, at lower concentrations of DNA we were able to confirm that the observed spacing between the DNA molecules occurred in intervals divisible by 200 nm (Figure 3F, lower panel), indicating that the 200 nm nanowells were functioning as expected. Similarly, we used Fourier transform (FT) analysis to verify the distribution patterns of the DNA within the curtains. As shown in Figure 3G, the peak-to-peak separation of the power spectrum from the FT correlated to within 5% of the expected values based on the designs of the barrier patterns. Taken together, these data demonstrate that the distance between adjacent nanowells dictates lateral separation between individual molecules that make up the DNA curtain.

As indicated above, DNA molecules aligned along smooth chromium barriers can slip laterally along the barrier edges, and this effect becomes more pronounced with shorter molecules of DNA. To illustrate this problem, either 48.5 kb  $\lambda$  DNA or a 23 kb PCR DNA fragment derived from the human  $\beta$ -globin locus was labeled with YOYO1 (see Materials and Methods) and these molecules were aligned along the edge of a smooth barrier. Kymograms illustrating the lateral locations of the DNA molecules over a period of 13.5 s were then generated from a cross-section of the curtain. As shown in Figure 4A, the fluorescently labeled molecules

exhibited movement consistent with lateral slippage of the DNA along the barrier edge even over periods spanning just a few seconds. In addition, quantification of the lateral motion (position variance divided by time) of the DNA molecules aligned along the smooth barrier edges yielded a broad range of values with a mean of  $1.6 \times 10^{-3} \pm 2.1 \times 10^{-3} \mu\text{m}^2/\text{s}$ . DNA curtains made using geometric barrier patterns with 500 nm spacing are shown in Figure 4B, along with the corresponding kymograms. In contrast to the movement observed with the smooth barriers, the  $\lambda$  DNA molecules aligned at the geometric patterns displayed absolutely no evidence of lateral slippage over the same 13.5 s period. Similar experiments with DNA molecules of sequentially shorter lengths revealed that the lateral movement of 34, 21, 11, and 5 kb DNA fragments was also eliminated with the geometric barrier patterns (Figure 4B). Quantification of the lateral motion of these DNA molecules yielded values of just  $2.00 \times 10^{-6} \pm 1.73 \times 10^{-6} \mu\text{m}^2/\text{s}$ , demonstrating that the DNA was effectively immobilized. These DNA molecules remained stationary even over much longer periods spanning tens of minutes and this was true for each of the different barrier dimensions (data not shown). This data provides conclusive evidence indicating that the geometric barrier patterns effectively restricted lateral movement of the DNA molecules along the barrier edges.

The number of DNA molecules that make up the curtains can be varied by modulating several different parameters, the simplest of which is the amount of DNA injected into the sample chamber.<sup>6,7</sup> If too much DNA is present, then multiple molecules of DNA will accumulate within each geometric nanowell. To avoid this problem these experiments can be conducted with a relatively low amount of DNA, such that less than one DNA molecule is expected per nanowell. This ensures that some of the nanowells will remain unoccupied, many of the wells will have a single DNA molecule, and some of the wells will have multiple DNA molecules. This can be confirmed by measuring the fluorescence intensity of the DNA in each well. For example, those nanowells harboring two molecules will be twice as bright as those harboring just one, therefore allowing for easy discrimination. Figure 5A shows sections of YOYO1-stained DNA curtains with differing amounts of DNA assembled at barriers with 1900 nm spacing between the adjacent geometric nanowells. These three images were collected from a single barrier set, as the design of the barriers themselves effectively provides a gradient of differing DNA concentrations. This occurs because the guide channel openings that direct the tethered DNA molecules to the nanowell-containing barriers are all similar widths, whereas the different tiers within the barrier set get incrementally wider.<sup>6</sup> Fluorescence cross-sections of the DNA molecules are shown in panel (B) and the relative signal intensity of corresponding to the different numbers of DNA molecules are indicated by the horizontal bars. Single DNA molecules were readily identified because they exhibited the lowest observed relative signal intensity (compare the upper, middle and lower panels in Figure 5A and B). Nanowells with multiple DNA molecules were also readily identified because they exhibited a clear incremental increase in the relative signal intensity consistent with 1 or more additional DNA molecules (compare the upper, middle, and lower panels in Figure 5B). Figure 5C shows a histogram of the number of DNA molecules per nanowell, demonstrating that under the conditions used for assembling the DNA curtains most of the nanowells (44%) contained only one molecule of DNA, whereas 8% had no DNA, 13% had 2 DNA molecules, 18% had 3 DNA molecules, and 17% had 4 or more molecules of DNA.

To further confirm the assignment of the lowest relative signal intensity as arising from just one DNA, the DNA molecules were partially digested in real time with very low concentrations of the restriction endonuclease *AvaI* (Figure 5D and E, and see below). If just one DNA molecule is present in a nanowell, then stochastic cleavage events will coincide with the complete and near instantaneous loss of any DNA downstream from the corresponding cleavage site because the YOYO1-stained DNA fragment liberated by the *AvaI* cut will be washed away by buffer flow. In contrast, if multiple DNA molecule are present in a single nanowell, then a single stochastic cleavage event by *AvaI* will not yield instantaneous loss of

all downstream signal, but rather will result in a decrease in signal intensity downstream of the cleavage site corresponding to loss of just one DNA molecule. As shown in Figure 5D, when a single DNA is loaded in the nanowell cleavage by the restriction enzyme leads to immediate loss of the corresponding downstream DNA fragment. In contrast, when multiple DNA molecules are present in a nanowell (Figure 5E; in this example there are two molecules in the nanowell), cleavage by the restriction enzyme results in an incremental decrease in the downstream signal because just one of the DNA molecules is cut over the course of the digest. The results from these partial restriction digests confirmed that the lowest YOYO1 fluorescence signal corresponds to just one molecule of DNA.

### Dynamic Optical Restriction Mapping

As shown above, these geometric barrier patterns permit studies of even relatively small DNA fragments by eliminating their lateral mobility along the barrier edges. We have also demonstrated that we can load the geometric nanowells with single DNA molecules. In previous work we have shown that the design of the curtains also yields DNA molecules that are all aligned with the same sequence orientation based upon the location of the biotin tag at a specific end of the DNA.<sup>6</sup> As a consequence of this consistent alignment, complete restriction digest of the DNA molecules within the curtain yields identical, tethered fragments whose lengths correspond to the furthest upstream cleavage site.<sup>6</sup> Complete digests at high concentrations of restriction enzyme can not be used to identify multiple sites cleaved by the same restriction enzyme because the downstream DNA is flushed from the sample chamber as soon as the DNA is cleaved. As shown above, restriction digests done at low concentrations of enzyme can reveal stochastic cleavage events, which in principle, could be used to reveal all of the fragments corresponding to each of these intermediate lengths. However, this is only true if the digest is viewed in real time, and sufficient numbers of molecules are observed to detect all sites, and the cleavage rate is slower than the data acquisition frequency. If these criteria are met, then following each individual cleavage event, the downstream fragment will be immediately flushed from the sample chamber by buffer flow, leaving behind the intact biotinylated fragment whose shortened length would correspond to the location of the cleavage site. This can happen repeatedly on the same DNA until that particular molecule is cleaved at the furthest upstream site relative to the anchored end of the DNA. The large number of DNA molecules that can be viewed with these DNA curtains makes it possible to detect all of the potential sites within the DNA, and the geometric nanowells prevent the DNA molecules from slipping back and forth after they are cleaved. Eventually all of the DNA molecules will be cut to a final length corresponding to the furthest upstream restriction site. We refer to this real time digest as dynamic optical restriction mapping and an example of such an assay is shown in Figure 6A and B, using the restriction enzymes *EcoRI* and *BamHI*, respectively. These kymograms were selected because they provide examples where each of the five *EcoRI* sites or five *BamHI* sites can be identified. The total time required for this digest was just under 120 s. This assay is not possible with smooth barrier designs because the DNA molecules start to rapidly slip back and forth as the fragment lengths become shorter and shorter, thus interfering with measurements of the same DNA molecule over time. Thus this real time dynamic optical restriction mapping assay is greatly facilitated when used in combination with barrier patterns comprised of the geometric nanowells.

### Discussion

Single-molecule microscopy has the potential to reveal details of reaction mechanisms and macromolecular dynamics previously inaccessible to traditional ensemble approaches. In an effort to make these techniques more broadly applicable we have used nanoscale engineering to establish a novel, high-throughput approach that we call DNA curtains, which facilitates massively parallel data acquisition from thousands of individual molecules viewed in real time.

Here we have shown that geometric barrier patterns can also be used to align curtains of DNA molecules tethered to a fluid lipid bilayer and that the geometry of the barriers can be used to dictate the lateral distance between the individual molecules that make up the curtains. These geometric barrier patterns are simple, yet highly effective at directing DNA molecules to defined locations on a surface, and we demonstrate that single molecules of DNA can be loaded into the geometric nanowells where they can be retained for further analysis and experimentation. This work brings the power of nanofabrication to bear on single-molecule biology by providing a very simple and robust means of controlling the lateral dispersion of DNA molecules assembled into a molecular curtain.

In our previous studies we demonstrated that DNA curtains are highly advantageous for analysis of protein-DNA interactions, particularly with systems that involve lateral movement of proteins along DNA.<sup>8,9</sup> Moreover, while our DNA curtain assays have a demonstrated capability to enable massively parallel data acquisition, evaluation of the resulting data remains a challenge because automated image analysis programs can not readily distinguish two or more identical objects if they overlap with one another. With the advent of the geometric barrier patterns these problems are eliminated. The DNA molecules are maintained at fixed distances from one another and we can verify that only one molecule is loaded in a particular well based on the fluorescence intensity of the labeled DNA and/or restriction digest of the DNA. The ability to load and retain individual DNA molecules into geometric nanowells portends the future possibility of individually handling or isolating these single molecules. We envision that the flexibility afforded by nanolithography will enable construction of intricate barrier patterns that can be used for even more complex manipulations of lipid anchored DNA molecules.

While the primary motivation for this work remains the development of robust, high-throughput tools for single-molecule optical detection of protein-DNA interactions, we envision that the DNA curtains and geometric nanowells have numerous potential applications pertaining to physical analysis of large DNA molecules. For example, an overarching aspect of genome research remains characterization of large DNA fragments, and numerous approaches have been developed for manipulating, analyzing, and isolating these molecules.<sup>16-20</sup> We have shown that DNA curtains made using geometric patterns can generate optical restriction maps of the tethered DNA molecules. Because these assays are performed in the context of a microfluidic system the cleaved DNA fragments can easily be isolated for further analysis. This type of real time restriction digest imaging can be used to rapidly map the DNA molecules. The large numbers of molecules aligned in the curtains ensures acquisition of statistically relevant data from just a single run.

## Acknowledgment

We thank Dr. James T. Yardley for valuable advice and suggestions throughout this work. We thank Dr. Ruben Gonzales and members of our laboratories for insightful discussions and carefully reading this manuscript. We thank Ilya Finkelstein for assistance with data analysis. This research was funded in part by the Initiatives in Science and Engineering (ISE; awarded to E.C.G. and S.W.) program through Columbia University, and by an NIH grant (GM074739) and an NSF PECASE Award to E.C.G. T.A.F. is a recent recipient of an NSF Graduate Research fellowship. This work was partially supported by the Nanoscale Science and Engineering Initiative of the National Science Foundation under NSF Award No. CHE-0641523 and by the New York State Office of Science, Technology, and Academic Research (NYSTAR).

## References

- (1). Bustamante C, Bryant Z, Smith SB. *Nature* 2003;421:423–7. [PubMed: 12540915]
- (2). Cairns BR. *Nat. Struct. Mol. Biol* 2007;14:989–96. [PubMed: 17984961]
- (3). Ha T. *Curr. Opin. Struct. Biol* 2001;11:287–92. [PubMed: 11406376]
- (4). Zlatanova J, van Holde K. *Mol. Cell* 2006;24:317–29. [PubMed: 17081984]



- (5). van Oijen AM. *Biopolymers* 2007;85:144–53. [PubMed: 17083118]
- (6). Fazio T, Visnapuu M-L, Wind S, Greene EC. *Langmuir*. 2008Epub (ahead of print)
- (7). Granéli A, Yeykal C, Prasad TK, Greene EC. *Langmuir* 2006;22:292–299. [PubMed: 16378434]
- (8). Gorman J, Chowdhury A, Surtees JA, Shimada J, Reichman DR, Alani E, Greene EC. *Mol. Cell* 2007;28:359–70. [PubMed: 17996701]
- (9). Prasad TK, Robertson RB, Visnapuu ML, Chi P, Sung P, Greene EC. *J. Mol. Biol* 2007;369:940–53. [PubMed: 17467735]
- (10). Prasad TK, Yeykal C, Greene EC. *J. Mol. Biol* 2006;363:713–728. [PubMed: 16979659]
- (11). Granéli A, Yeykal C, Robertson RB, Greene EC. *Proc. Natl. Acad. Sci. U.S.A* 2006;103:1221–1226. [PubMed: 16432240]
- (12). Tsai J, Sun E, Gao Y, Hone JC, Kam LC. *Nano Lett* 2008;8:425–30. [PubMed: 18205424]
- (13). Boxer SG. *Curr. Opin. Chem. Biol* 2000;4:704–9. [PubMed: 11102877]
- (14). Cremer PS, Boxer SG. *J. Phys. Chem. B* 1999;103:2554–2559.
- (15). Groves J, Boxer S. *Acc. Chem. Res* 2002;35:149–57. [PubMed: 11900518]
- (16). Bensimon A, Simon A, Chiffaudel A, Croquette V, Heslot F, Bensimon D. *Science* 1994;265:2096–2098. [PubMed: 7522347]
- (17). Dimalanta ET, Lim A, Runnheim R, Lamers C, Churas C, Forrest DK, de Pablo JJ, Graham MD, Coppersmith SN, Goldstein S, Schwartz DC. *Anal. Chem* 2004;76:5293–5301. [PubMed: 15362885]
- (18). Lebofsky R, Bensimon A. *Brief. Funct. Genom. Proteom* 2003;1:385–396.
- (19). Lin J, Qi R, Aston C, Jing J, Anantharaman TS, Mishra B, White O, Daly MJ, Minton KW, Venter JC, Schwartz DC. *Science* 1999;285:1558–1562. [PubMed: 10477518]
- (20). Riehn R, Lu MC, Wang YM, Lim SF, Cox EC, Austin RH. *Proc. Natl. Acad. Sci. U.S.A* 2005;102:10012–10016. [PubMed: 16000405]

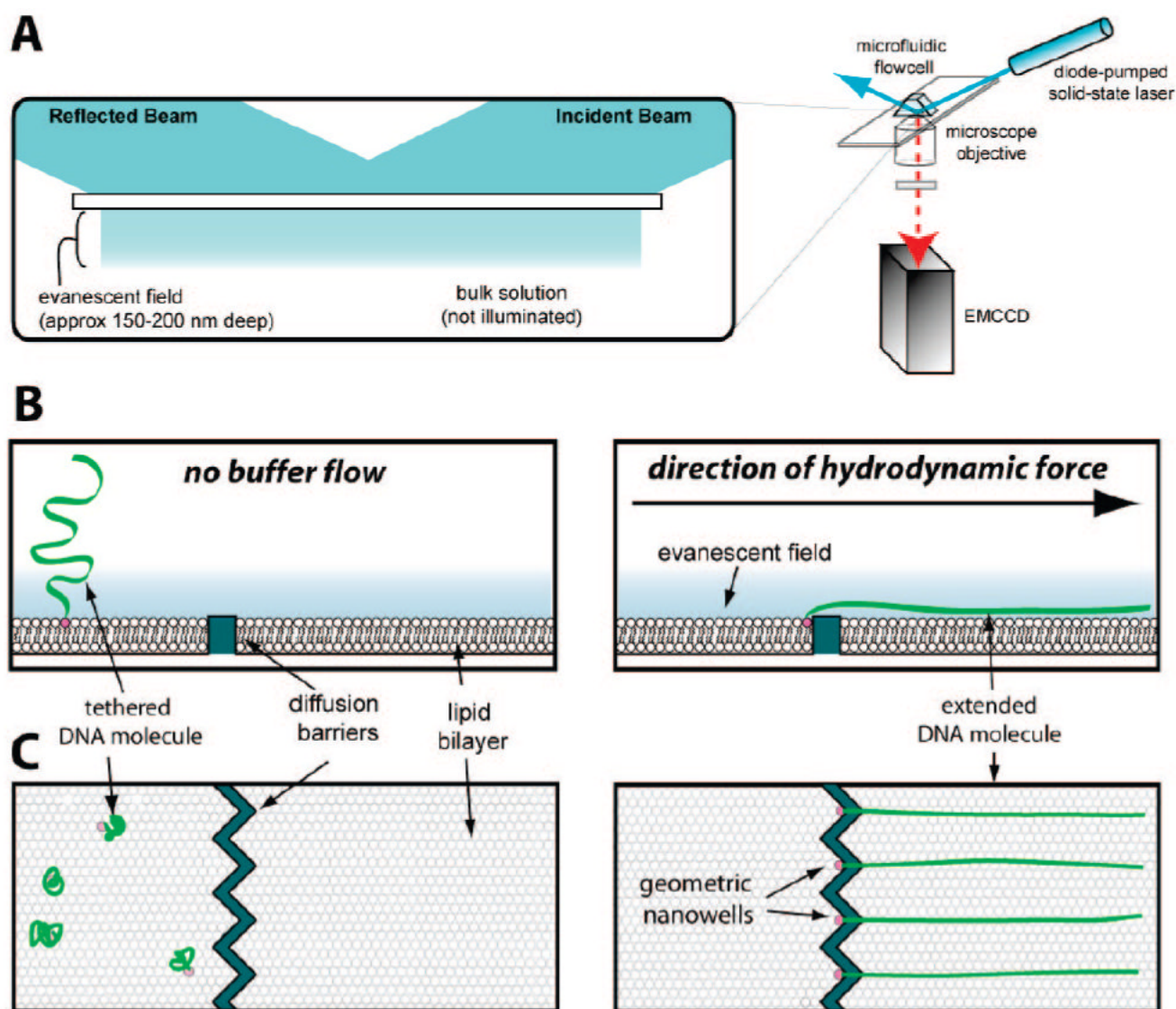


**Figure 1.** Design strategy for geometric nanowells. Panel (A) shows a simplified schematic of the TIRFM microscope and the illumination geometry used to generate the evanescent field. To make DNA curtains, the surface of a fused silica sample chamber is coated with a supported lipid bilayer and DNA molecules are anchored by one end to lipids within the bilayer. Panel (B) shows an illustration of the surface viewed from the side in the presence and absence of buffer flow (right and left panels, respectively). The barriers engineered on the surface disrupt the bilayer and the DNA molecules accumulate against their edges when flow is applied. The pattern of the geometric barrier is revealed when viewed from above (C), and the DNA molecules are expected to load into the vertices of the adjacent triangles.

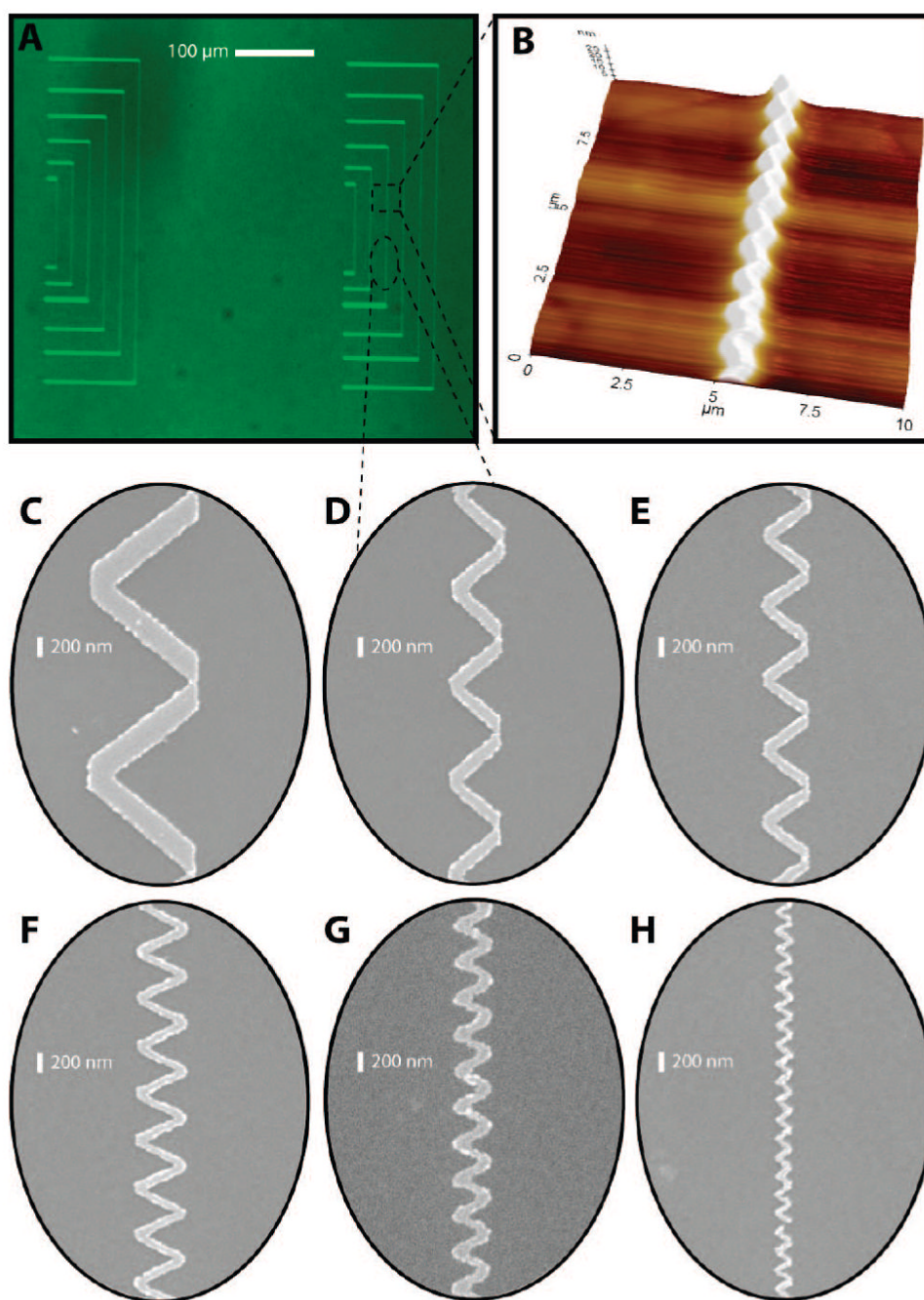


**Figure 2.** Images of diffusion barriers with geometric nanowells. Panel (A) shows an optical image collected at 10× magnification of two barrier patterns in which the parallel barriers are made in a sawtooth pattern to form the geometric nanowells. Panel (B) shows an AFM image of a  $10 \times 10 \mu\text{m}^2$  area of fused silica with a 20 nm tall chromium barrier with a representative geometric pattern that repeats at 1- $\mu\text{m}$  intervals. SEM images of typical chromium barriers viewed from above are shown in panels (C-H). The peak-to-peak distances of these patterns are 1900, 1000, 750, 500, 350, and 200 nm, for (C-H), respectively; all SEM images are shown at the same magnification and a 200 nm scale bar is indicated in each for reference.

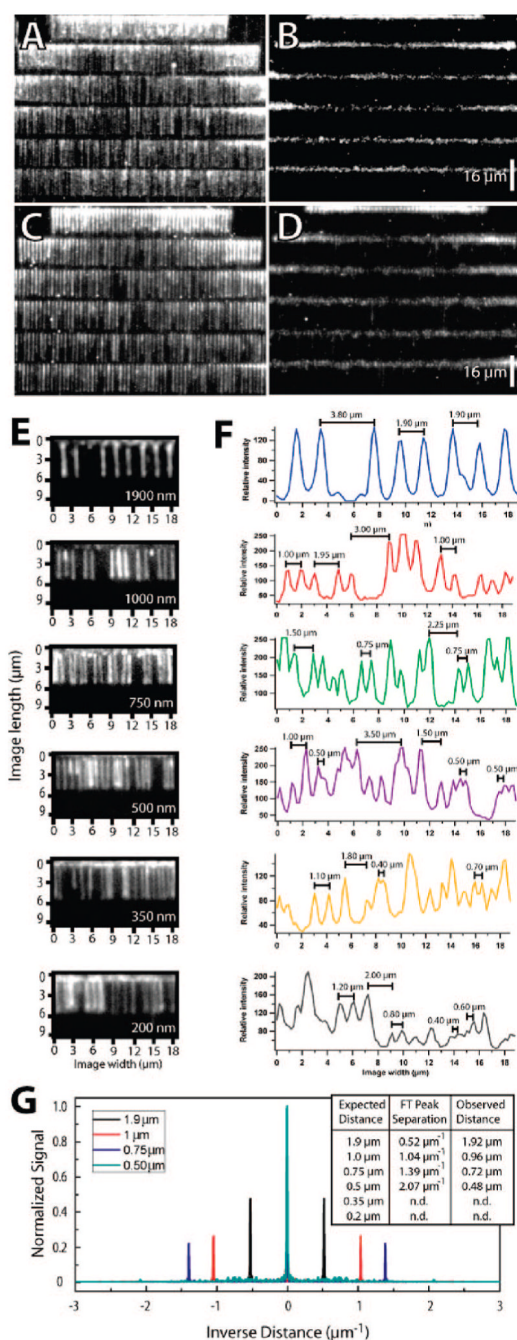


**Figure 3.** DNA curtains with different separation distances. Panels (A) and (B) show examples of DNA curtains assembled at barriers with 1000 nm spacing, in the presence of buffer flow and immediately after pausing flow, respectively. The molecules are 48.5 kb  $\lambda$  DNA stained with YOYO1. Panels (C) and (D) show DNA curtains assembled at barriers with 1900 nm spacing, in the presence of buffer flow and immediately after pausing flow, respectively. The different panels in (E) show typical examples of sections from YOYO1-stained DNA curtains prepared using geometric barrier patterns with spacings of 1900, 1000, 750, 500, 350, and 200 nm, as indicated. The DNA molecules used here are 23kb PCR products derived from the human  $\beta$ -globin locus. Fluorescence cross-sections of the same curtains are shown in panel (F) and the

distances between some representative examples of adjacent DNA peaks are indicated in micrometers. These images were collected from single flow cells containing different sets of nanowell barriers with the indicated spacing. Panel (G) shows a normalized power spectrum of Fourier Transforms from cross-sections of DNA curtains made using geometric barrier patterns with spacings of 1900, 1000, 750, and 500 nm. Note that the optical resolution was insufficient to perform this analysis on the 350 and 200 nm barrier patterns. Values for the expected distance based on the barrier design, the peak separation found by the FT analysis, and the corresponding observed separation distance are all indicated (inset).

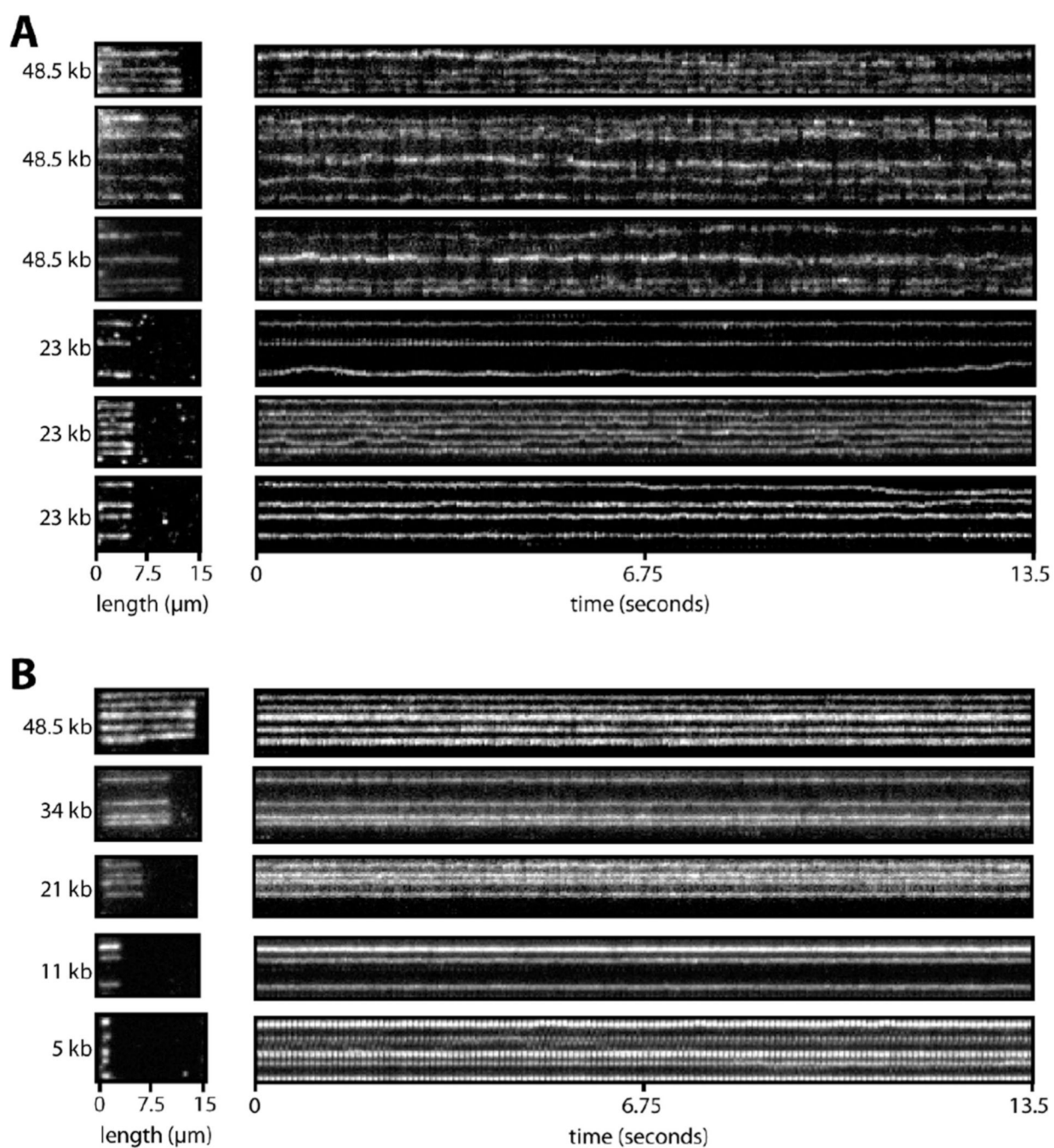


**Figure 4.**

DNA slippage is eliminated with geometric barrier patterns. The left panels in (A) show single 100-ms images of a section from different DNA curtains assembled at a smooth barrier edge. The YOYO1 stained molecules are comprised of either 48.5 kb  $\lambda$  DNA or a 23 kb PCR product, as indicated. The right panels in (A) show kymograms of cross-sections from the same images spanning a duration of 13.5 s, illustrating the lateral slippage of the DNA molecules along the barrier edges. The left panels in (B) show a DNA curtain assembled at a geometric barrier with 500 nm spacing. The lengths of the DNA molecules were 48.5, 34, 21, 11, and 5 kb, as indicated, and the fragments smaller than the 48.5 kb  $\lambda$ -DNA were generated by restriction digest of  $\lambda$  using NheI, EcoRI, PvuI, and SphI, respectively. The right panels in (B) show 13.5 s

kymograms demonstrating that the lateral motion of these DNA is eliminated with the geometric barrier patterns.

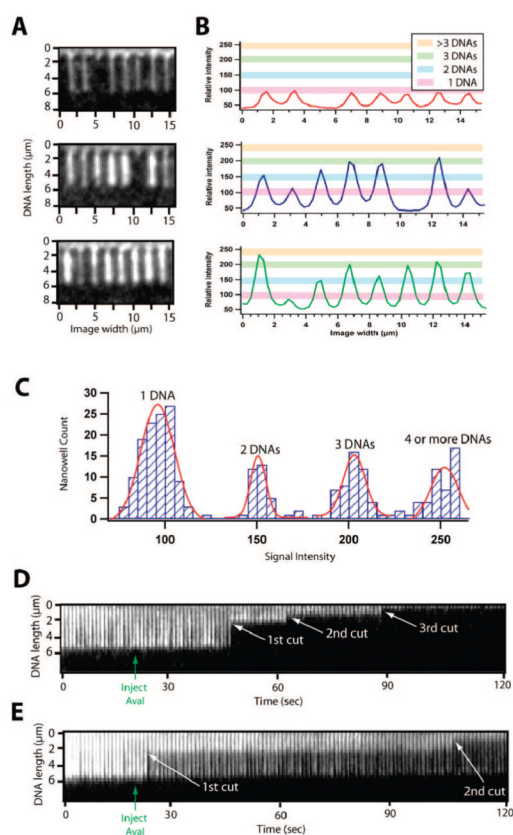


**Figure 5.**

Loading single DNA molecules into the nanowells. Panel (A) shows examples of DNA curtains assembled with different DNA densities at barriers with  $1.9 \mu\text{m}$  spacing between the nanowells. Fluorescence cross-sections of the same images are shown in panel (B) and the colored bars highlight the relative fluorescence signal intensity (in arbitrary units) observed for different numbers of DNA loaded per nanowell, either 1, 2, 3, and  $>3$  DNAs as indicated. The histogram in (C) shows the distribution of DNA occupancy within the nanowells. Under the conditions used here, 44% of the nanowells were loaded with a single DNA molecule. Panel (D) shows a real time *AvaI* restriction digest of a single DNA molecule loaded into a geometric nanowell, along with the corresponding graph of signal intensity taken from the indicated cross-section of the kymogram. The injection of *AvaI* is indicated with a green arrow and the individual DNA cleavage events are indicated with white arrows. Note that there are three *AvaI* cut sites in the 23kb DNA, but only a subset are cut here because of the low concentration on enzyme injected. Panel (E) shows the results of the same *AvaI* digest when two DNA molecules are loaded into a single nanowell. Here the first cleavage event causes reduction, but not complete loss of the downstream YOYO1 signal.



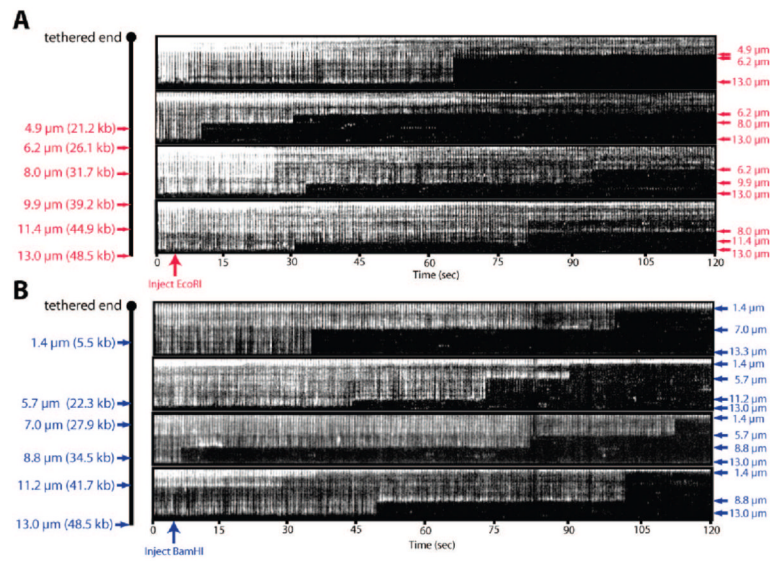


**Figure 6.** Dynamic optical restriction mapping with *EcoRI* and *BamHI*. Kymograms in panels (A and B) show representative examples of real time restriction digests of the  $\lambda$  phage genome using either *EcoRI* or *BamHI*. A schematic of  $\lambda$  is shown at the left; the tethered end of the DNA is indicated as are the predicted cleavage sites in kilobases (kb) and the observed fragment lengths in micrometers ( $\mu\text{m}$ ).